Relationships among North American deer based on mitochondrial DNA and ultraconserved elements, with comments on mito-nuclear discordance

Lukas B. Klicka
 Peru State College

Nadje Najar
 University of California Riverside

Hernan Vázquez-Miranda
 National Autonomous University of Mexico: Universidad Nacional Autonoma de Mexico

Robert Zink (✉ rzink2@unl.edu)
 University of Nebraska-Lincoln   https://orcid.org/0000-0001-9243-4567

Abstract

Despite their economic, cultural, and ecological significance, the phylogenetic relationships among North American deer remain uncertain, due in part to discordance between phylogenies built from mitochondrial DNA (mtDNA) and nuclear markers. However, the data from these two genomic regions have heretofore been analyzed in isolation. We compared phylogenies built from mtDNA Cyt *b*, and single nucleotide polymorphisms (SNPs) from the mitogenome and nuclear (ultraconserved elements, UCEs) markers from the same individuals to investigate mito-nuclear discordance within and between taxa in the genus *Odocoileus*. A Cyt *b* tree shows haplotype sharing between *O. hemonius* and *O. virginianus*. Mitochondrial DNA SNPs separated *O. hemionus* and *O. virginianus*, whereas nuclear SNPs separated *O. hemionus*, O. *virginianus*, *O. v. couesi*, *O. v. clavium* and *O. h. sitkensis* plus *O. h. columbianus*. We found less support for *O. h. columbianus* as a distinct taxon, which had signs of introgression with nominate *O. h. hemionus*. The well-established paraphyly of mtDNA haplotypes from *O. virginianus* and *O. hemonius* is confirmed with comparisons of mtDNA and nuclear-encoded SNPs from the same individuals. A possible reason for mito-nuclear discordance is that the evolutionary splits are relatively recent, the mtDNA results are influenced by genome capture via ancient hybridization, or ancestral lineage sorting; we think our UCE data favor the latter explanation. Niche models suggested allopatric refugia at the Last Glacial maximum for these taxa except for a parapatric or sympatric distribution estimated for mule deer and black-tailed deer, which might explain the modern hybrid zone.

Introduction

Molecular data revolutionized evolutionary studies in the late 20th Century, providing novel insights into topics ranging from higher level phylogenies to phylogeography. Paradoxically, the evolution of charismatic megafauna such as bears (genus *Ursus*; Cronin et al. 2014), elephants (genus *Loxodonta*; Roca et al. 2005) and North American canids (genus *Canis*; Hailer and Leonard 2008) has proven difficult to elucidate with molecular data due to hybridization, molecular marker bias, and mito-nuclear incompatibilities, which obscure species limits and complicate conservation strategies. Deer of the genus *Odocoileus* represent another such case.

Despite their economic, cultural, and ecological importance, relationships among the *Odocoileus* deer have proven difficult to parse. White-tailed deer (*O. virginianus*) range widely through North America and include up to 65 described subspecies (Smith 1991, Heffelfinger 2011), two of which are noteworthy: Coues deer (*O. v. couesi*) and the endangered Florida Key deer (*O. v. clavium*). Mule deer (*O. hemionus*) occur in western North America and have been divided into as many as 11 subspecies, including the Columbian black-tailed deer (*O. h. columbianus*) and Sitka black-tailed deer (*O. h. sitkensis*). How these taxa are related to each other, and species vs subspecies limits, are open questions.

Mule deer and white-tailed deer are generally distinguishable by morphology, although they are known to hybridize (Cathey et al. 1998, Bradley et al. 2003). Early attempts to distinguish species using mitochondrial DNA (mtDNA) restriction sites in a hybrid zone revealed asymmetric gene flow, with female white-tailed deer more commonly mating with male mule deer than the reverse cross (Carr et al. 1986). Hopken et al. (2015) found that mtDNA control region sequences separated most, but not all, white-tailed deer and mule deer in a small area of the Pacific Northwest. A phylogeny of genera and species of American deer based on mtDNA Cyt *b* sequences could not separate mule and white-tailed deer, which shared several mtDNA haplotypes (Gutiérrez et al. 2017). However, the extent of geographic sampling is of interest. Gutiérrez et al. (2017) used samples of *O. hemionus* represented a broad part of the range and included eight subspecies (*hemionus*, *crooki*, *sheldoni*, *fuliginatus*, *inyoensis*, *peninsulae*, *californicus*, *eremicus*). In contrast, the samples of *O. virginianus* used by Gutiérrez et al. (2017) represented a relatively small part of the range, with one sample of *O. v. couesi* from Chihuahua and no samples of *O. v. clavium*. Their mtDNA tree separated most black-tailed deer (*O. h. columbianus* and *O. h. sitkensis*) from mule deer similar to Cathey et al. (1998), but samples of *O. h. columbianus* from Oregon, and *O. virginianus* from Texas and the District of Columbia were included with mule deer. The single individual of Coues deer was sister to a single *O. h. crooki* from Texas. The remaining *O. h. columbianus and O. h. sitkensis* were shown as sister to *Mazama pandora* (Yucatan brown brocket deer), instead of *O. virginianus*; however, the low bootstrap support on their tree suggests this relationship is uncertain.

Analysis of markers from the nuclear genome have confirmed broad genomic differentiation between mule deer and white-tailed deer with evidence for hybridization where their ranges overlap (Combe et al. 2022). Using Y-linked gene sequences, Cathey et al. (1998) found a better correlation between nuclear DNA and morphology, finding black tailed deer and mule deer as sister taxa, indicating that maternal gene flow from white-tailed to mule deer had biased phylogenetic inference. Latch et al. (2009, 2014)

analyzed 10 microsatellite loci in 1900 individuals sampled across the range of black-tailed deer and mule deer. Their results confirmed the phylogeographic and taxonomic split between mule deer and black-tailed deer, although they (Latch et al. 2011) also reported a hybrid swarm between mule deer and Columbian black-tailed deer. Based on PRNP gene sequences, Vázquez-Miranda and Zink (2020) found three synonymous and diagnostic single nucleotide polymorphism (SNP) substitutions between mule deer and white-tailed deer, and Zink et al. (2020) reported three F1 hybrids between mule deer and white-tailed deer from Nebraska. Villanova et al. (2017) found that Key deer and those from the neighboring county of Collier in south Florida had mtDNA profiles that were distinct from mainland whitetails, although their STRUCTURE plot based on 12 microsatellite loci did not show complete separation, which might reflect the longer coalescence times of nuclear loci. Lastly, a population study restricted to western Kansas where mule deer and white-tailed deer overlap employed genome-wide SNPs and was able to sort unequivocally both species despite hybridization (Combe et al. 2022).

Wright et al. (2022) analyzed mtDNA Cyt *b* sequences, including many of those used by Gutiérrez et al. (2017), and concluded that there had been at least two instances of mtDNA genome capture between white-tailed and mule deer, which could explain the lack of species distinctiveness between the two species in mtDNA gene trees; they discounted hybridization and recent speciation. Wright et al. (2022) concluded that the most recent putative capture event occurred 1.32 million years ago. We are concerned whether a single mitochondrial DNA gene such as Cyt *b* can provide valid divergence dates as ascribed by Wright et al. (2022) given rate heterogeneity over time (Nakamoto et al. 2021) and an incomplete fossil record. Heffelfinger and Latch (2023) concluded that mtDNA genotype sharing between mule deer and white-tailed deer was as yet unexplained.

In this paper, we analyzed mtDNA sequences, and Single Nucleotide Polymorphisms (SNPs) derived from Ultraconserved Elements (UCEs) from multiple localities across North America to determine the best hypothesis for relationships among these cervid taxa. Our goal is to describe relationships among the major taxa, not to provide definitive taxonomic resolution at the subspecies level or below. To explore putative mito-nuclear conflicts reported by earlier studies and the hypothesis of mtDNA genome capture (Wright et al. 2022), we provide an explicit comparison of SNPs obtained from the same individuals for the mitogenome and nuclear genome. In addition, we use niche modeling (Peterson 2001) to explore whether major taxa were allopatric at the Last Glacial Maximum, which would suggest that evolutionary divergences predated and were maintained across this time period.

Methods

MtDNA Data and Phylogenetic Analyses

We downloaded Cyt *b* sequences (959 bp) for many of the same individuals used by Gutiérrez et al. (2017) but added more samples (see appendix for individuals and localities) from Vázquez-Miranda and Zink (2020): *O. virginianus* (n = 212), *O. v. couesi* (10), *O. v. clavium* (n = 34), *O. hemionus* (216), *O. h. sitkensis* (6), *O. h. columbianus* (42). We removed redundant haplotypes leaving 219 individuals: *O. virginianus* (n = 48), *O. v. couesi* (6), *O. v. clavium* (n = 1), *O. hemionus* (124), *O. h. sitkensis* (3), *O. h. columbianus* (37). We used the reduced Cyt *b* data set to generate a consensus maximum likelihood tree from 100 standard bootstraps (Hoang et al. 2018) with IQTREE (Minh et al. 2020), which determines the best-fit nucleotide substitution model (Kalyaanamoorthy et al. 2017). We computed the average genetic distance among major taxa using DnaSP (Rozas et al. 2017). We extracted the mitochondrial genome from the UCE data by aligning to *O. hemionus* mitochondrial genome (NCBI reference NC_020729.1) with bcftools (Li et al. 2009). We concatenated 659 mtDNA SNPs and used PAUP* 4.0a169 (Swofford 2023) to infer a tree using the SVDQuartets routine using the multispecies coalescent with 200 bootstrap replicates. To evaluate further the differentiation between taxa and the hypothesis of mitochondrial DNA capture (Wright et al. 2022), we used IQTREE (as above) to construct a maximum likelihood tree from their Cyt *b* data after converting sequences into amino acids to determine if phylogenetic haplotype mixing was a result of synonymous nucleotide changes.

Ultraconserved Elements, Population and Phylogenetic Analyses

Our samples included white-tailed deer from Minnesota (n = 5), New York (n = 5), Nebraska (N = 17), mule deer from Nebraska (n = 11) and California (n = 1), Coues deer from Arizona (n = 5), Key deer (n = 5), black-tailed deer from California (n = 7), and black-tailed deer from Alaska (n = 4). We extracted the tissue samples from hunter-harvested animals using a Qiagen kit, whereas frozen museum samples (Coues, Key, Alaskan black-tails; see acknowledgments) were extracted using phenol-chloroform to ensure comparable DNA concentrations from tissue loans. We sent purified DNA in the desired concentration to RAPiD Genomics where

library preparation using the UCE Tetrapods 5Kv1 kit (targeting 5060 loci; Faircloth et al. 2012) was performed for Illumina sequencing using their high-throughput workflow with proprietary chemistry. Briefly, DNA was sheared to a mean fragment length of 400bp, fragments were end-repaired, followed by incorporation of unique dual-indexed Illumina adapters and PCR enrichment. Samples were pooled equimolar and sequenced 2x150bp.

We checked read depth and quality with FastQC and removed two samples with low coverage. We removed adapter sequences and assembled reads (forwards and reverse) using PEAR (Zhang et al. 2014) and then aligned samples with to a deer reference genome (ovis_v1.0) with BWA (Li and Durbin 2009). We converted BAM files with bcftools (Li et al. 2009) to VCF files and then filtered SNPs by quality (minQ = 20), percent missing data (--max-missing 0.5), and minor allele frequency (--maf 0.05).

We recovered over 125,877 total SNPs from the nuclear genome. We thinned nuclear SNPs to 10% and removed sites with high linkage disequilibrium, resulting in a set of 12,587 SNPs for analysis. We concatenated all SNPs into one sequence. To examine any bias that may have been introduced by down sampling the SNPs, we generated a random dataset of the same size (12,587) and the complete dataset of ~ 126K SNPs with Discriminant Analysis of Principal Components (DAPC; Jombart et al. 2010). The DAPC analyses of different datasets did not conflict.

We estimated a species tree topology using SVDquartets (Chifman & Kubatko, 2014; Wascher & Kubatko, 2020) in PAUP* v. 4.0a169 (Swofford, 2023), sampling all possible quartets on a consensus sequence of concatenated nuclear (12,587) SNPs using 100 bootstrap replicates; the multispecies coalescent was enforced. In addition, we completed a RAxML v8.2.11 (Stamatakis 2014) analysis with a GTR + Gamma model of evolution and 500 bootstrap replicates, which was consistent with the SVDQuartets analysis and results are not shown here.

We used STRUCTURE v2.3.4 (Pritchard et al. 2000) to assess genetic clustering among individuals. We initially evaluated genetic structure from 58 samples. For this, we completed 10 independent runs for models that ranged in population values (K) from 1–7. Each independent run was for 700,000 generations with the first 200,000 generations used as burn-in. After we evaluated the likelihood scores for the population models and the ΔK (Evanno et al. 2005) calculation we determined that it was appropriate to split the dataset into eastern (*O. virginianus*, *O. v. clavium*, *O. v. couesi*) and western samples (*O. h. columbianus* and *O. h. sitkensis*). The eastern (N = 36) and western (N = 22) datasets were each evaluated with a predetermined number of populations (K) from 1–5. Each population model was run independently 10 times for 700,000 generations, 200,000 as burn-in.

Comparison of phylogenetic patterns in SNP from mitochondrial and nuclear genomes

To compare phylogenetic hypotheses based on SNPs from the mitogenome and nuclear genome, we input the mtDNA SNP data into IQTree and PAUP4 and compared the likelihoods of the two trees using the Shimodaira-Hasegawa (2000) test. We also did the reciprocal analysis (genomic SNP data on the two trees).

Niche models

To ascertain if *O. hemionus* and *O. virginianus* and their component subspecies groups were allopatric at the Last Glacial Maximum (LGM) we constructed ecological niche models for each of the taxa. In brief, niche models show where the climate conditions used by a species today existed at some other time (e.g., LGM), assuming that the species would occur in these areas (Peterson 2001, Peterson et al. 2011). We extracted locality information from the Global Biodiversity Information Facility (https://www.gbif.org) into Maxent (Elith et al. 2011; Phillips et al. 2006) to build a climatic niche model that was then projected onto the 19 LGM climate layers at the LGM (Hijmans et al. 2005; CCSM model); we used default parameters with the exception that we used 1000 iterations to assist model convergence. Point samples per taxon were: *O. virginianus* (2499), *O. v. clavium* (436), *O. v. couesi* (916), *O. h. hemionus* (2494), *O. h. columbianus* (1999), and *O. h. sitkensis* (421). We estimated the receiver operating characteristic (ROC) for each model using 15% of the data for testing. For each model, we selected climate variables from an initial run with greater than 5% contribution to the model, and then repeated the Maxent analysis with 10 replicates. We visualized estimated average distributions of the 10 replicates with DIVA-GIS using the 10% probability threshold to depict presence or absence (Hijmans et al. 2012). Our goal in niche modeling was to discover potential LGM refugia, reasoning that irrespective of when divergence among taxa occurred, maintenance of genetic differences between taxa would require allopatric refugia at the LGM.

Results

MtDNA

The average sequence divergence (*p*) for Cyt *b* between all white-tailed deer and mule deer was 0.026. IQtree selected the HKY + F + I + G4 substitution model, calculated the proportion of invariable sites as 0.5393, and estimated the gamma shape alpha as 1.048. Samples of *O. hemionus* and *O. virginianus* are intermingled on the Cyt *b* tree (Fig. 1). A grouping of individuals representing *O. v. couesi* included an individual identified as *O. h. crooki* (Genbank: FJ188885) apparently from Texas (Latch et al. 2009) that might be misidentified. The single individual of *O. v. clavium* (representing 34 total individuals with an identical haplotype; see Villanova et al. 2017) is embedded within a clade of *O. virginianus*. A clade of *O. h. columbianus* includes interspersed individuals identified as *O. h. sitkensis*. A clade of *O. hemionus* included individuals from Alberta, Arizona, British Columbia, Utah, Nevada, Wyoming, Idaho and Oregon. One clade included *O. h. hemionus*, *O. h. columbianus*, and *O. virginianus* (from Nebraska). Thus, apart from *O. v. couesi* and *O. v. clavium*, the mtDNA gene tree does not reflect current taxonomy.

The SVDquartets tree (Fig. 2) for the 659 concatenated SNPs (469 parsimony informative) from the mitogenome with 100 bootstrap replicates, basically separated only white-tailed deer and mule deer, although not perfectly. The maximum likelihood tree (Supplementary Figure S1) for Cyt *b* amino acids separated the sequences into several apparent groups (none with significant bootstrap support) including a paraphyletic cluster of white-tailed deer, a group of mule/black-tailed deer that included two white-tailed deer, and a second cluster of mule/black-tailed deer that included seven white-tailed deer (red branches in figure).

Ultraconserved Elements

A phylogenetic hypothesis based on UCE data separates *O. hemionus* and *O. virginianus* and shows clades including *O. v. couesi* and *O. v. clavium* (Fig. 3). Samples of *O. h. sitkensis* are reciprocally monophyletic and are sister to *O. h. columbianus* (from California), whereas other *O. h. columbianus* occur elsewhere on the *O. hemionus* side of the tree. A STRUCTURE plot separates white-tailed deer and mule deer (Fig. 4a). When the data are analyzed within these two species, there is incomplete separation between mule deer, Sitka black-tailed deer, and Columbian black-tailed deer from California (Fig. 4b), whereas *O. v. couesi*, *O. v. clavium*, and *O. h. sitkensis* are independent (Fig. 4c).

Niche models

Based on percentage contribution to the initial models, ROC values and climate layers used for each taxon were as follows: *O. virginianus* (0.86; 5,6,12,17,18); *O. v. couesi* (0.99; 3,4,15,18,19); *O. v. clavium* (0.98; 2,3,4,6,7,14); *O. hemionus* (0.88, 3,9,18); *O. h. sitkensis* (0.99, 2,5,7 14,19); *O. h. columbianus* (0.95, 8,15,18,19). The niche models for Coues, Key and white-tailed deer suggest non-overlapping distributions at Last Glacial Maximum (Online Resource 1a,b). Sitka black-tailed deer were apparently separated from Columbian black-tailed deer and mule deer, the latter two of which appear to have broadly overlapping LGM distributions (Online Resource Fig. 2a, 2b).

Discussion

The UCE tree (Fig. 3) supports the distinctiveness of *O. v. virginianus*, *O. v. couesi*, *O. v. clavium*, *O. h. sitkensis*, *O. h. columbianus* (from California), and *O. h. hemionus*, in contrast with the mtDNA tree (Fig. 1, Supplementary Figure S1). The STRUCTURE analyses (Fig. 4), however, show incomplete separation of mule deer and black-tailed deer, which is consistent with the hybrid swarm noted by Latch et al. (2011); our lack of mule deer outside of Nebraska prevents definitive conclusions about range-wide patterns in this taxon. Combe et al. (2022) reported a hybridization rate of nearly 10% between white-tailed deer and mule deer in western Kansas (eight of 92 individuals), the state immediately to the south of Nebraska (see Russell et al. 2021, Wright et al. 2022). However, our data suggest a lower frequency of hybrids in Nebraska (e.g., Zink et al. 2020).

Translocations of deer by game managers likely affected the genetic structure of many game species, such as wild turkey (*Meleagris gallopavo*) and mallards (*Anas platyrhynchos*) (Mock et al. 2004, Schummer et al. 2023). Regarding white-tailed deer, Chafin et al. (2021) commented that "an unintended consequence was that natural patterns of gene flow became obscured and pretranslocation signatures of population structure were replaced." This suggests that documenting the history of white-tailed deer

populations will require examination of historical museum specimens and a thorough sampling of modern deer populations with dense genomic data.

Mito-nuclear discordance.--The lack of species distinctiveness between mule deer and white-tailed deer in the mtDNA tree (Fig. 1; Supplementary Figure S2) conflicts with the monophyly of these two species in the UCE tree (Fig. 3) and a PRNP gene tree (Zink et al. 2020). Because previous assessments of mito-nuclear discordance were based on data sets including different individuals, we confirmed mito-nuclear discordance by analyzing SNPs from the mitogenome and nuclear genome for the same individuals. Because white-tailed deer and mule deer are closely related, a mtDNA gene tree with its four times more rapid coalescence time should capture the species split relative to a nuclear gene tree (Zink and Barrowclough 2008), although it does not. This mito-nuclear mismatch could have several causes, including ongoing introgression or retention of ancestral alleles. Wright et al. (2022) suggest that white-tailed deer diverged from black-tailed deer, with mule deer later splitting from black-tailed deer. They concluded that a history of hybridization led to at least one genome capture of white-tailed deer mtDNA by mule deer at 1.32 mybp. Their samples are more widely distributed geographically than ours, which precludes a strong test of their genome-capture hypothesis. In contrast, Heffelfinger and Latch (2023) considered hypotheses of dispersal, hybrid origin, and isolation in glacial refugia as causes of the mito-nuclear discord between mule deer, white-tailed deer and black-tailed deer and noted that none of these could be ruled out, other than noting that a common mechanism across hypotheses is ancestral lineage sorting. Our nuclear SNP tree (Fig. 3) is not consistent with a genome-capture event (Wright et al. 2022) and suggests that white-tailed deer and mule deer split first, with black-tailed deer subsequently diverging from mule deer. In addition, given the 1.32 my since the putative mtDNA capture, gene flow ought to have spread the mis-matched mtDNA genotypes much farther than observed by Wright et al. (2022). Hence, we suggest that the mito-nuclear mismatch between mule deer and white-tailed deer is best explained as ancestral lineage sorting that has yet to be completed, although ongoing hybridization will result in new mismatches.

Lineages and glacial history.--Our niche models (Online Resource 1,2) suggest that the distinctiveness of the taxa in *O. virginianus* was at least present and maintained through the LGM via largely allopatric refugia. Our UCE data are insufficiently dense to capture the hybrid zone between *O. h. columbianus* and *O. h. hemionus* (Latch et al. 2011). However, a hybrid zone could explain the apparent overlapping or parapatric LGM distribution (Fig. S2a,b) of the latter two taxa and could explain their intermingled mtDNA genetics (Fig. 1) discussed above.

Taxonomic implications.-- We conclude that the best estimate of the species tree (see Heckeberg 2020) is best based on the UCE data (Figs. 3,4). Most authors recognize white-tailed deer and mule deer as distinct species (Bradley e al. 2014; Ramírez-Pulido et al. 2014; Caire et al. 2019), which is consistent with our results. Key deer are distinct in both mtDNA and nuDNA trees. Hence, Key deer could be recognized as a separate species based on their reciprocal monophyly in the UCE tree, although they are not entirely distinct at a few microsatellite loci (Villanova et al. 2017). Similarly, Coues deer appears to be distinct and worthy of consideration for species status. Bradley et al. (2014) considered black-tailed deer and mule deer to be conspecific, but UCE data and the SNPs from the mitogenome suggest they are evolving independently. Latch and Heffelfinger (2022) found genetic support for two black-tailed deer subspecies (*O. h. columbianus*, *O. h. sitkensis*) and mainland *O. h. hemionus* and the two island subspecies, (*O. h. cerrosensis* on Cedros Island and *O. h. sheldoni* on Tibur´on Island). Our data also indicate that Sitka black-tailed deer are distinct and reciprocally monophyletic, whereas we found less support for *O. h. columbianus*. We suggest that none of the other samples from named subspecies diverge to the degree of these taxa, suggesting that the remaining subspecies nomenclature of both mule deer and white-tailed deer does not reflect evolutionary diversity. We acknowledge that greater sampling is required to determine if discrete taxonomic boundaries exist, although if the hypothesis of mtDNA genome capture is correct (Wright et al. 2022), mtDNA could obfuscate taxonomic decisions.

Declarations

References

1. Bradley RD, Ammerman LK, Baker RJ, Bradley LC, Cook JA, Dowler RC, Jones C, Schmidly DJ, Stangl FB, Van Den Bussche RA, Würsig BG (2014) Revised checklist of North American mammals north of Mexico. Museum of Texas Tech University.

2. Caire W, Loucks LS, Haynie ML, Coyner BS, Braun JK (2019) Updated and revised checklist of the mammals of Oklahoma. In Proc OK Acad Sci 99:1-6.

3. Carr SM, Ballinger SW, Derr JN, Blankenship LH, Bickham JW (1986) Mitochondrial DNA analysis of hybridization between sympatric white-tailed deer and mule deer in west Texas. Proc Nat Acad Sci 83:9576-9580.

4. Cathey JC, Bickham JW, Patton JC (1998) Introgressive hybridization and nonconcordant evolutionary history of maternal and paternal lineages in North American deer. Evol 52:1224-9.

5. Chafin TK, Zbinden ZD, Douglas MR, Martin BT, Middaugh CR, Gray MC, Ballard JR, Douglas ME (2021) Spatial population genetics in heavily managed species: Separating patterns of historical translocation from contemporary gene flow in white-tailed deer. Evol Appl https://doi.org/10.1111/eva.13233.

6. Chifman J, Kubatko L (2014) Quartet inference from SNP data under the coalescent model. Bioinformatics 30:3317-3324.

7. Combe FJ, Jaster L, Ricketts A, Haukos D, Hope AG (2022) Population genomics of free-ranging Great Plains white-tailed and mule deer reflects a long history of interspecific hybridization. Evol Appl 15:111-131.

8. Cronin MA, Rincon G, Meredith RW, MacNeil MD, Islas-Trejo A, Cánovas A, Medrano JF (2014) Molecular phylogeny and SNP variation of polar bears (*Ursus maritimus*), brown bears (U. arctos), and black bears (U. americanus) derived from genome sequences. J Hered 105:312-23.

9. Elith J, Phillips SJ, Hastie T, Dudık M, Chee YE, Yates CJ (2011) A statistical explanation of MaxEnt for ecologists. Diver Dist 17:43–57.

10. Evanno G, Regnaut S, Goudet J (2005) Detecting the number of clusters of individuals using the software STRUCTURE: a simulation study. Mol Ecol 14:2611-2620.

11. Faircloth BC, McCormack JE, Crawford NG, Harvey MG, Brumfield RT, Glenn TC (2012) Ultraconserved elements anchor thousands of genetic markers spanning multiple evolutionary timescales. Syst Bio 61 717-726.

12. Gutiérrez EE, Helgen KM, McDonough MM, Bauer F, Hawkins MT, Escobedo-Morales LA, Patterson BD, Maldonado JE (2017) A gene-tree test of the traditional taxonomy of American deer: the importance of voucher specimens, geographic data, and dense sampling. ZooKeys 697:87-131.

13. Hailer F, Leonard JA (2008) Hybridization among three native North American *Canis* species in a region of natural sympatry. PLoS one. 2008 Oct 8;3(10):e3333.

14. Hellelfinger, J (2011) Taxonomy, evolutionary history, and distribution. Pp. 3-42, in Biology and Management of White-tailed Deer, D. G. Hewitt, ed. CRC Press.

15. Heffelfinger JR, Latch EK (2023) Origin, classification, and distribution. In Ecology and Management of Black-Tailed and Mule Deer In North America. Heffelfinger JR and Krausman PR, eds. In Press.

16. Hijmans RJ, Cameron SE, Parra JL, Jones PG, Jarvis A (2005) Very high resolution interpolated climate surfaces for global land areas. Int. J Climatol 25:1965–1978.

17. Hijmans RJ, Guarino L, Mathur P (2012) DIVA-GIS. Version. 7.5. http://www.diva-gis.org/.

18. Hopken MW, Lum TM, Meyers PM, Piaggio AJ (2015) Molecular assessment of translocation and management of an endangered subspecies of white-tailed deer (*Odocoileus virginianus*). Cons Genet 16:635-47.

19. Jombart T, Devillard S, Balloux F (2010) Discriminant analysis of principal components: a new method for the analysis of genetically structured populations. BMC Genet 11:1-5.

20. Kalyaanamoorthy S, Minh BQ, Wong TK, Von Haeseler A, Jermiin LS (2017) ModelFinder: fast model selection for accurate phylogenetic estimates. Nat Meth 14:587-589.

21. Latch EK, and Heffelfinger JR (2022). Genetics informs meaningful intraspecific taxonomy: the black-tailed and mule deer complex. Animal Production Science.

22. Latch EK, Heffelfinger JR, Fike JA, Rhodes Jr, OE (2009) Species-wide phylogeography of North American mule deer (*Odocoileus hemionus*): cryptic glacial refugia and postglacial recolonization. Mole Ecol 18:1730-1745.

23. Latch EK, Kierepka EM, Heffelfinger JR, Rhodes Jr, OE (2011) Hybrid swarm between divergent lineages of mule deer (*Odocoileus hemionus*). Mole Ecol 20:5265-5279.

24. Latch EK, Reding DM, Heffelfinger JR, Alcalá-Galván CH, Rhodes Jr, OE (2014) Range-wide analysis of genetic structure in a widespread, highly mobile species (*Odocoileus hemionus*) reveals the importance of historical biogeography. Mole Ecol 23:3171-3190.

25. Li H, Durbin R (2009) Fast and accurate short read alignment with Burrows-Wheeler Transform. Bioinfor 25:1754-60. [PMID: 19451168]

26. Li H, Handsaker B, Wysoker A, Fennell T, Ruan J, Homer N, Marth G, Abecasis G, Durbin R (2009) The sequence alignment/map format and SAMtools. Bioinfor 25:2078-79.

27. Minh BQ, Schmidt HA, Chernomor O, Schrempf D, Woodhams MD, von Haeseler A, Lanfear R (2020) IQ-TREE 2: New models and efficient methods for phylogenetic inference in the genomic era. Mol Biol Evol 37:1530-1534. https://doi.org/10.1093/molbev/msaa015

28. Mock K, Latch E, Rhodes OE (2004) Assessing losses of genetic diversity due to translocation: long-term case histories in Merriam's turkey (*Meleagris gallopavo merriami*). Cons Genet 5:631.

29. Nakamoto, A, Harada M, Mitsuhashi R, Tsuchiya K, Kryukov AP, Shinohara A, Suzuki H (2021) Influence of Quaternary environmental changes on mole populations inferred from mitochondrial sequences and evolutionary rate estimation. Zoo Let 7:1-11.

30. Peterson A (2001) Predicting species' geographic distributions based on ecological niche modeling. The Condor 103:599–605.

31. Peterson AT, Soberón J, Pearson RG, Anderson RP, Martínez-Meyer E, Nakamura M, Araújo MB (2011). Ecological niches and geographic distributions. Princeton, NJ: Princeton Univ. Press

32. Phillips SJ, Anderson RP, Schapire RE (2006) Maximum entropy modeling of species geographic distributions. Ecol Model 190:231-259.

33. Pritchard JK, Stephens M, Donnelly P (2000) Inference of population structure using multilocus genotype data. Genet 155:945-959.

34. Ramírez-Pulido J, González-Ruiz N, Gardner AL, Arroyo-Cabrales J (2014) List of recent land mammals of Mexico. https://repository.si.edu/bitstream/handle/10088/33974/2014%20List%20of%20recent%20land%20mammals%20Mexico.pdf?sequence=1&isAllowed=y

35. Roca AL, O'Brien SJ (2005) Genomic inferences from Afrotheria and the evolution of elephants. Curr opin genet devel 15:652-659.

36. Rozas J, Ferrer-Mata A, Sánchez-DelBarrio JC, Guirao-Rico S, Librado P, Ramos-Onsins SE, Sánchez-Gracia, A (2017) DnaSP v6. DNA sequence polymorphism analysis of arge datasets. Mol Biol Evol 34: 3299-3302.

37. Russell T, Cullingham C, Ball M, Pybus M, Coltman D (2021) Extent and direction of introgressive hybridization of mule and white-tailed deer in western Canada. Evol Appl 14:1914-25.

38. Schummer ML, Simpson J, Shirkey B, Kucia SR, Lavretsky P, Tozer DC. (2023) Population genetics and geographic origins of mallards harvested in northwestern Ohio. Plos one. 2023 Mar 15;18(3):e0282874.

39. Shimodaira H, Hasegawa M (2001) CONSEL: for assessing the confidence of phylogenetic tree selection. Bioinformatics.17:1246-1247.

40. Smith WP (1991) *Odocoileus virginianus*. Mamm Sp 388: 1–13.

41. Stamatakis A (2014) RAxML version 8: a tool for phylogenetic analysis and post-analysis of large phylogenies. Bioinfor 30:1312-1313.

42. Swofford DL (2023) PAUP*: Phylogenetic Analysis Using PAUP, version 4.0a 169. https://paup.phylosolutions.com/.

43. Vázquez-Miranda H, Zink RM (2020) Geographic distribution of chronic wasting disease resistant alleles in Nebraska, with comments on the evolution of resistance. J Fish Wildl Man 11: 46-55.

44. Villanova VL, Hughes PT, Hoffman EA (2017) Combining genetic structure)re and demographic analyses to estimate persistence in endangered Key deer (*Odocoileus virginianus clavium*). Cons Genet 18:1061-1076.

45. Wascher M, Kubatko L (2020) Consistency of SVDQuartets and maximum likelihood for coalescent-based species tree estimation. Syst Biol 70:33-48.

46. Wright EA, Roberts EK, Platt RN, Bayouth JV, Conway WC, Bradley RD (2022) Mitochondrial capture and subsequent genetic divergence generates a novel haplogroup: evidence from ancient and ongoing hybridization in mule and white-tailed deer. Journal of Mammalogy.

47. Zhang J, Kobert K, Flouri T, Stamatakis A (2014) PEAR: a fast and accurate Illumina Paired-End reAd mergeR. Bioinformatics 30:614-620.

48. Zink RM, Barrowclough GF (2008) Mitochondrial DNA under siege in avian phylogeography. Mole Ecol 17:2107-2121.

49. Zink RM, Najar N, Vázquez-Miranda H, Buchanan BL, Loy D, Brodersen BW (2020) Geographic variation in the PRNP gene and its promoter, and their relationship to chronic wasting disease in North American deer. Prion 14:185-192.
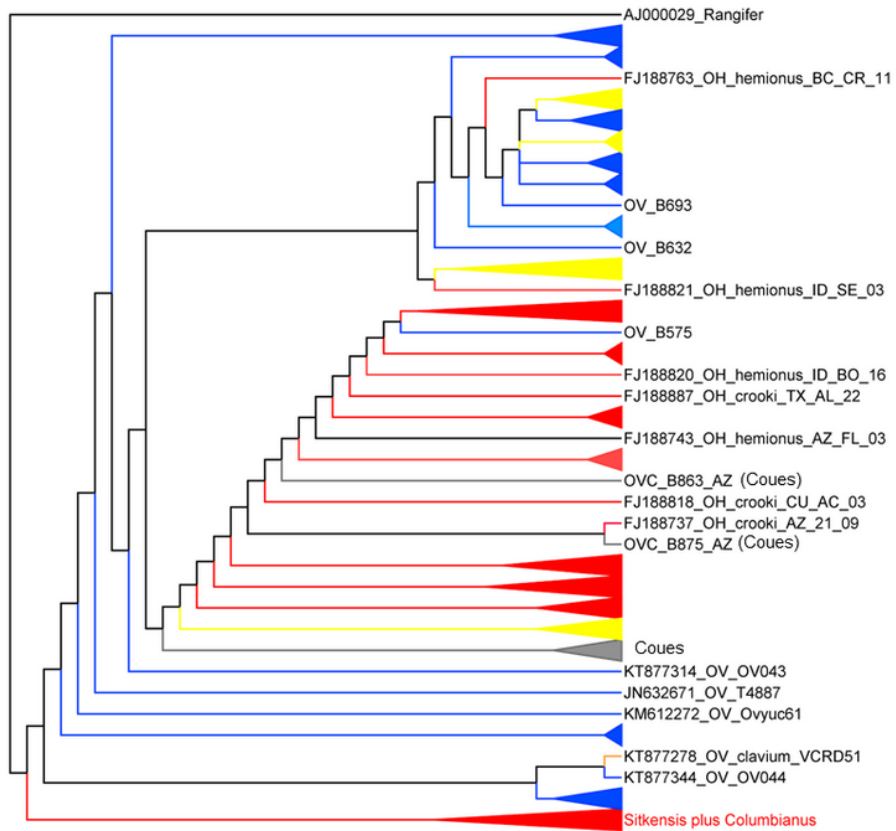
Figures

Figure 1

Condensed maximum likelihood phylogeny based on 959 bp of cytochrome *b*. Red = mule deer, blue = white-tailed deer, yellow = individuals of both mule deer and white-tailed deer, black = Coues deer. Triangular terminal taxa with no labels signify multiple individuals corresponding to the color code. No nodes had bootstrap values that exceeded 75%. Node labels preceded by a letter start Genbank sequence identifiers, and the others are either in Gutiérrez et al. (2017) or the appendix.
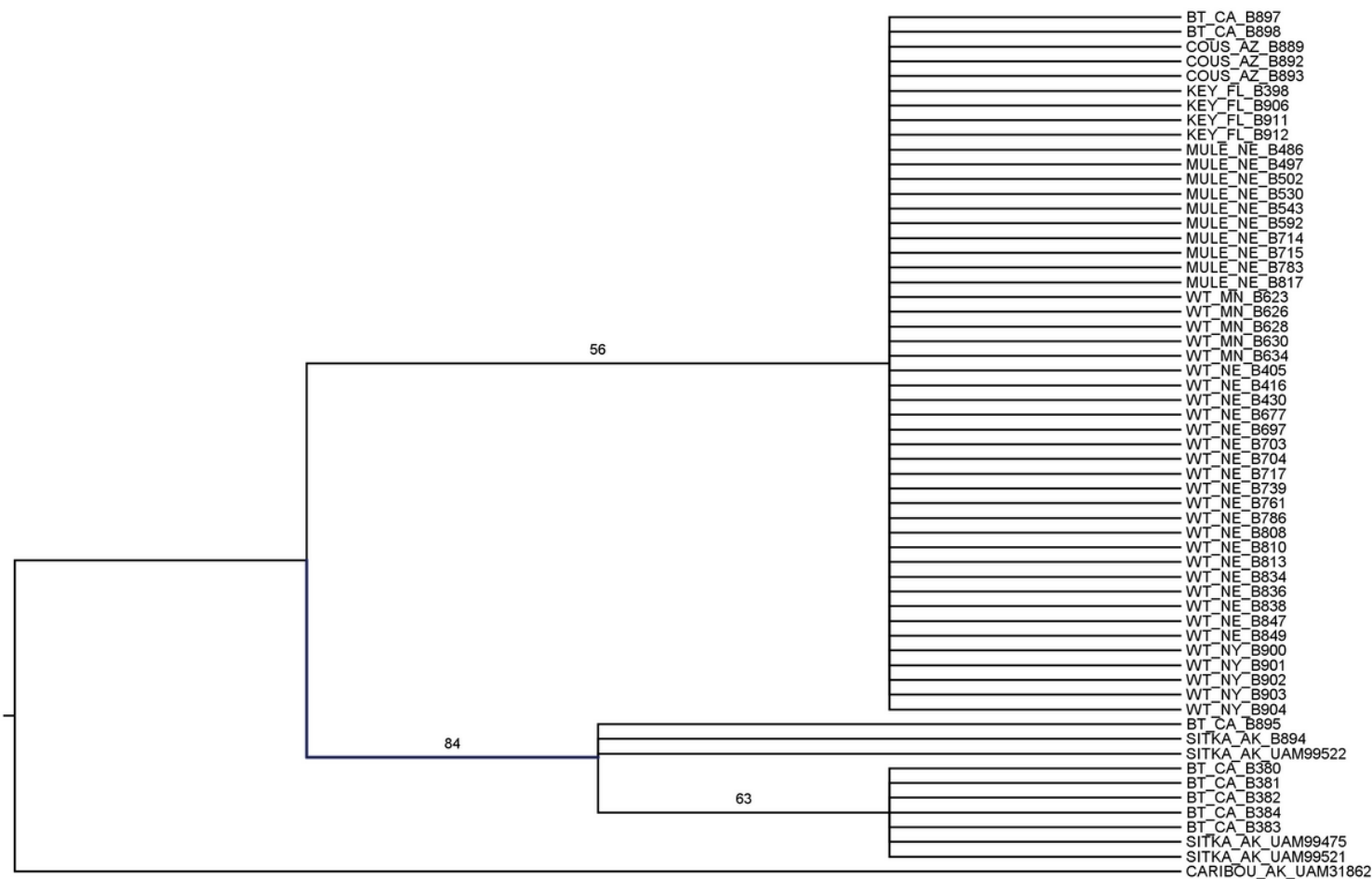
Figure 2

SVDQuartets tree for 659 SNPs from the mitogenome (including Cyt *b*). Numbers on branches are bootstrap support values (out of 100 replicates).
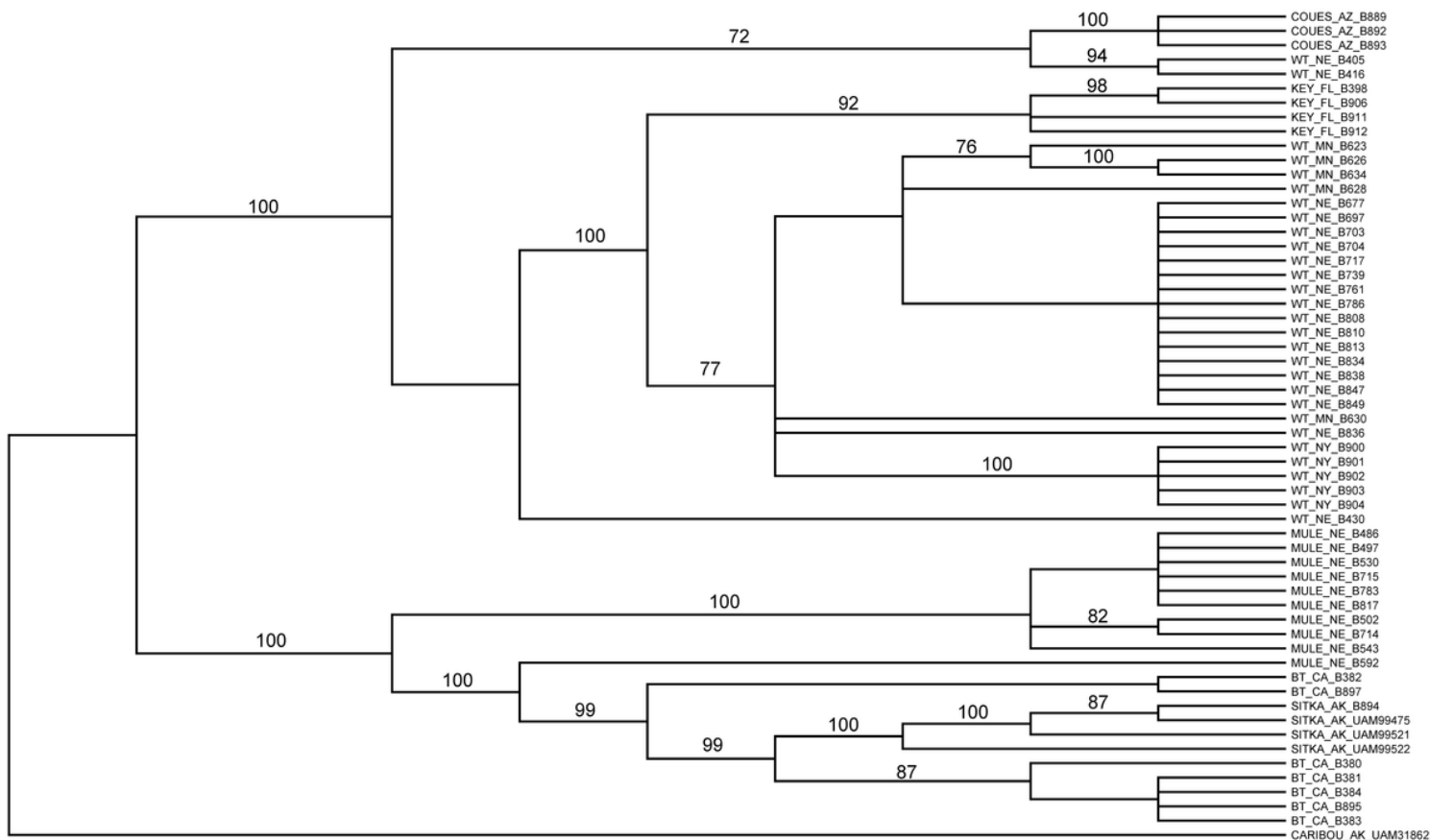
Figure 3

SVDquartets phylogeny using a concatenated dataset of nuclear SNPs (12,587) and a consensus sequence for each individual with bootstrap values (out of 100 replicates) greater than 70 shown on branches.
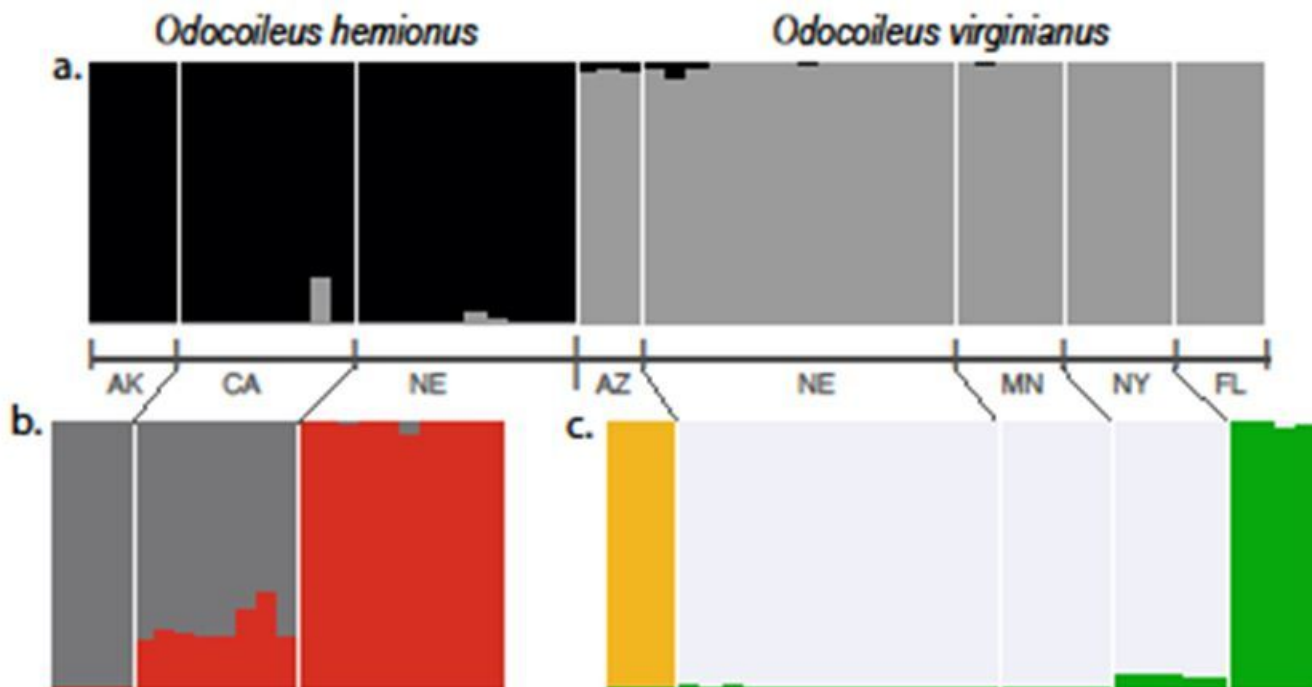
Figure 4

a. STRUCTURE results for the population model (K=2) that received the most support with all individuals included. **b.** The model that received the highest support was K=2 when only *O. hemionus* individuals were analyzed. **c.** The STRUCTURE results receiving the highest support for *O. virginianus* samples was a population model of K=3 corresponding to white-tailed deer, Coues deer and Key deer. Individual columns represent the proportional population assignments for individuals and abbreviations are as follows: AK–Alaska, CA–California, NE–Nebraska, AZ–Arizona (Coues deer), MN–Minnesota, NY–New York, FL–Florida (Key deer).

Supplementary Files

This is a list of supplementary files associated with this preprint. Click to download.

- OnlineResourcesAndAppendix.docx